ORIGINALARBEIT

# Single-sweep-based methods to improve the quality of auditory brain stem responses Part I: Optimized linear filtering

*Michael Granzow, Helmut Riedel, Birger Kollmeier*
AG Medizinische Physik, Carl-von-Ossietzky-Universität, D-26111 Oldenburg

**Abstract** *This study is a systematic evaluation of the influence of different filter settings on the quality of auditory brain stem responses performed on a single sweep basis, i.e., on a post-hoc analysis of all unaveraged single epochs. For purposes of comparison, a quality analysis was also carried out when only two sub-averages were known. The question of optimal lower and upper filter edge frequencies is addressed for monaural and binaural stimuli at 20, 40 and 60 dB (nHL) for different recording sites. Only linear (finite impulse response) filters were used. Filter edge frequencies of 30–50 Hz and 1300–1700 Hz are to be recommended for practical purposes. These values are independent of the stimulation level and recording site. In comparison with average-based quality estimates, the single-sweep approach was found to be superior, as is confirmed both by the practical examples and by theoretical observations.*

*Key words:* *Auditory brain stem responses*
*filter cut-off frequencies*
*optimal filtering*
*single sweeps*
*residual noise*

Corresponding author: Prof. Dr. med. Dr. rer. nat. Birger Kollmeier
AG Medizinische Physik, Universität Oldenburg, D-26111 Oldenburg
Phone: +49 441 7985466
Fax: +49 441 7983698
E-mail: birger.kollmeier@uni-oldenburg.de

# Einzelepochenbasierte Methoden zur Verbesserung der Qualität früher akustisch evozierter Potentiale Part I: Optimale lineare Filter

*Michael Granzow, Helmut Riedel, Birger Kollmeier*
AG Medizinische Physik, Carl-von-Ossietzky-Universität, D-26111 Oldenburg

**Zusammenfassung** *In dieser Studie wird der Einfluss der Grenzfrequenzen des Hochpass- und Tiefpassfilters auf die Qualität früher akustisch evozierter Potenziale untersucht, die auf Einzelepochenbasis geschätzt wird. Zum Vergleich wird die Qualitätsanalyse auch durchgeführt, wenn nicht alle Einzelepochen, sondern nur zwei Teilmittelwerte bekannt sind. Es werden monaurale und binaurale Stimuli, drei Pegel (20, 40 und 60 dB nHL), sowie verschiedene Elektrodenpositionen betrachtet. Es finden nur phasenlineare FIR-Filter Verwendung. Filtergrenzfrequenzen von 30 bis 50 Hz und 1300 bis 1700 Hz können für die Praxis empfohlen werden. Diese Werte sind unabhängig vom Pegel und der Elektrodenposition. Die Qualitätsschätzung auf Einzelepochenbasis ist der mittelwertbasierten Schätzung überlegen. Dies zeigt eine theoretische Betrachtung ebenso wie die praktischen Beispiele.*

*Schlüsselwörter:* *Frühe akustisch evozierte Potenziale*
*Filtergrenzfrequenzen*
*Optimale Filter*
*Einzelepochen*
*Reststörung*

## 1. Introduction

The extraction of small signals from intense background noise is a common problem in many applications and has received considerable attention over the years. In the case of auditory brain stem responses (ABR), the situation is further complicated by the fact that recording frequently has to be done quickly, leaving little room for sophisticated on-line or off-line noise-reduction techniques. However, such techniques are highly desirable in order to minimize the measurement time for a given quality of the recorded averaged signal or to optimize the quality for a given measurement time. In the present study we therefore test and optimize various signal processing techniques that are based on the recording and evaluation of each single sweep. In doing so, we assume that computational costs for storing and processing the large amount of unaveraged data is not an issue. Rather, the complete information found in the raw data is exploited. In order to show the advantage of this technique, we compare the single-sweep-based estimates of signal quality with the traditional method of comparing two averages, either obtained by repeating the experiment or averaging alternately into two buffers.

Two methods are mainly applied to the raw signals (an ensemble of epochs[1] of EEG responses to click-stimuli recorded with as little filtering as possible): digital linear-phase filtering of the individual epochs and/or the assignment of weightings to the epochs. These weightings are based on an estimate of the contamination of the sweeps by noise before averaging across the ensemble. These two procedures actually address two different aspects of the problem of noise reduction. The objective of this first part of the study is to systematically determine the optimal choice of filters for auditory brain stem recordings. A comparison of the averaging techniques is carried out in part II (*Riedel* et al. 2001).

It is meaningful to filter the raw data if the spectral composition of the signal component of the recorded sweeps is different from that of the noise component. The validity of this assumption for ABR has been demonstrated in a number of studies (*Doyle* and *Hyde* 1981a; *Møller* 1988; *Mühler* and *von Specht* 1996). However, the question of optimal filter cut-off frequencies still remains and will be dealt with in the present study. Although the literature is rich with advice against the use of analogue filters (*Janssen* et al. 1986; *Boston* and *Ainslie* 1980; *Doyle* and *Hyde* 1981a; *Tietze* and *Kevanishvili* 1990, including Bessel filters, *Doyle* and *Hyde* 1981b) and digital infinite impulse response (IIR) filters (*Doyle* and *Hyde* 1981a; *Elton* et al. 1984), linear (or zero) phase highpass filters are recommended with edge frequenc-ies of 100 (*Doyle* and *Hyde* 1981a), 200 (*Boston* and *Ainslie* 1980; *Tietze* and *Kevanishvili* 1990), and up to 400 Hz (*Mühler* and *von Specht* 1996). Given this multitude of contradicting recommendations, we will give reasons for so many different »optimal« filter settings having been found by different investigators, and put forward our own recommendation.

[1] We use the terms »sweep« and »epoch« interchangeably.

## 2. Methods

### 2.1 Subjects

Nine male subjects ranging in age from 25 to 35 years were recruited from the staff of the Medical Physics Group at the University of Oldenburg, Germany. They reported no hearing problem and were judged to have normal hearing on the basis of routine clinical audiometry (audiometric loss less than 10 dB at frequencies below 4 kHz and less than 15 dB at higher frequencies).

### 2.2 Stimuli

Rarefaction click stimuli were produced by applying rectangular voltage pulses of 100 $\mu$s duration to Etymotic Research ER-2 insert phones. The inter-stimulus interval between clicks was uniformly distributed between 60 and 80 ms, yielding an average stimulation rate of approximately 14.3 clicks per second. The monaural thresholds in quiet for a click train of one-second duration were determined individually by a 3-alternative forced-choice method with a 2-down 1-up scheme and averaged across subjects and ears. This level – referred to as 0 dB normal hearing level (nHL) – corresponds to 32 dB peak equivalent sound pressure level (p.e. SPL)[2].

### 2.3 Recordings

During the ABR recordings, the subjects lay in a sound shielded and electrically shielded room. They were instructed to relax and lie as comfortably as possible. Responses to monaural left, monaural right, and binaural stimulation at levels 20, 40, and 60 dB nHL (52, 72, and 92 dB p.e. SPL, respectively) were recorded for all subjects. No-stimulus recordings were also performed in order to study the frequency composition of the EEG background noise. Three channels were recorded simultaneously with a Synamps 5803 differential amplifier. Scalp activity was recorded from the left mastoid (M1), the right mastoid (M2), and the forehead (Fz) with respect to the common reference electrode at the vertex (Cz). The ground electrode was placed at Fpz (all

[2] A sinusoid of frequency 1 kHz with the same peak-to-peak-amplitude showed 32 dB SPL on a Brüel & Kjær (B&K) amplifier type 2610 at a scale of SA 0252. The calibration was performed using an artificial ear (B&K type 4152) with a 2 cc coupler and an ER1-07 adapter for the insert earphones, a one-inch microphone (B&K 4144) and a preamplifier (B&K 2639).

electrode names as defined in the ten-twenty system, *Jasper* 1957). Electrode impedances were held well below 5 kΩ, typically between 1 and 2 kΩ at a 30 Hz test signal.

The signals were preamplified by a factor of 150 inside the shielded room and further amplified by the main amplifier by a factor of 83.3, yielding a total amplification of 82 dB. The amplified signals were passed through an analogue second-order antialiasing lowpass filter (12 dB per octave) with a cut-off frequency of 2 kHz. The filtered signals were digitized with 16 bits at a sampling rate of 10 kHz. The voltage resolution was approximately 6.7 nV per bit. The recording interval comprised 350 samples for each channel during a time interval of -11.0 to 24 ms relative to stimulus onset. Individual sweeps were collected for every stimulus condition $J$ = 10.000 and stored to hard disk without passing through any *digital* filters.

The amplifier is completely DC coupled and therefore allows DC recordings. DC correction can be done automatically and manually during the recording. The automatic correction took place if the voltage in at least one channel the voltage reached 70 % of the saturation value of the AD converter, which was ±220 $\mu$V. Thus it was no longer necessary to highpass filter the signals during the recording. This is very important because highpass filters introduce much more severe phase shifts than lowpass filters. During the recording, an artifact threshold of ±200 $\mu$V was used to avoid the storage of clipped sweeps. The speed of the voltage drift depended on the impedances and the muscular activity of the subjects, and showed inter-individual differences.

### 2.4 Filtering

The processing of the raw data primarily comprises linear filtering and averaging. The order of both operations is interchangeable due to their linearity, but only if no weighting or artifact rejection is used. Since a high DC value or drift of the epochs can thwart any meaningful weighting, all single epochs were filtered before a decision about exclusion or assignment of weightings was made. For this part of the study, unweighted averages were calculated using an artifact threshold of ±10 $\mu$V to the filtered epochs. The various averaging schemes employed are described in detail in the second part of this study (*Riedel* et al. 2001).

There are two advantages from filtering the ABR offline. First, it is possible to apply different filters to the same set of data and to determine an optimal filter. Secondly, it is known that IIR filters, and especially IIR highpasses, which are commonly used during ABR recordings, introduce waveform distortions and peak shifts due to their frequency-dependent group delay, see e.g., *Dawson* and *Doddington* (1973), *Boston* and *Ainslie* (1980), *Doyle* and *Hyde* (1981a, 1981b), *Elton* et al. (1984), *Janssen* et al. (1986). Symmetrical finite impulse response (FIR) filters, on the other hand, have a constant, i.e., frequency-independent group delay, and therefore do not distort, but only delay the waveform. This delay amounts to half the length of the impulse response of the FIR filter (*Oppenheim* and *Schaefer* 1989) and can be easily corrected.

To obtain a sufficient steepness, FIR filters with 200 taps and an attenuation of 6 dB at the corner frequencies were employed. They were generated with the window design method using a Hamming window. In order to obtain usable filtered data in an interval containing the ABR (-1 to 14 ms), the recording interval had to be extended by 20 ms (200 samples), i.e., to the range from -11 to 24 ms. Thus, the computational cost for clean filtering is enormous, since more than half of the data has to be recorded only for this purpose. Before passing a sweep through a FIR filter, a baseline voltage is subtracted from the whole sweep to avoid the step response of the filter being added to the sweep. Highpass cut-off frequencies were varied between zero and 100 Hz in steps of 10 Hz, lowpass cut-off frequencies from 100 to 2000 Hz in steps of 100 Hz. Edge frequencies higher than 2000 Hz were not used for the *digital* lowpass because this is the cut-off frequency of the analogue lowpass filter in the recording apparatus.

Processing and analysis tools were written in Matlab.

### 2.5 Evaluation of data quality

We compared two methods of data quality estimation: one based on averages, the other on single sweeps.

It is common clinical practice to store only a (non-weighted) average. An estimate of the signal-to-noise ratio (SNR) is then obtained by repeating the measurement or by averaging alternately into two buffers yielding two sub-averages, each consisting of $J$/2 epochs. The more similar they appear, the better the quality of the data and the higher the SNR will be. By denoting the filtered epochs with the odd number $x_o$ and epochs with the even number $x_e$ the sub-averages as a function of time $t$ are:

$$s_o(t) = \frac{1}{J/2} \sum_{o=1,3,\ldots}^{J-1} x_o(t), \qquad s_e(t) = \frac{1}{J/2} \sum_{e=2,4,\ldots}^{J} x_e(t) \quad (1)$$

An attempt to estimate the residual noise $\sigma_{oe}$ can be done in terms of the difference of the two sub-averages:

$$\sigma_{oe}(t) = \frac{1}{2}\left(s_o(t) - s_e(t)\right). \quad (2)$$

This concept was proposed as the »plus-minus reference« by *Schimmel* (1967) and later used by *Wong* and *Bickford* (1980) as the »plus-minus average«.

In the case of non-weighted averaging, the signal estimate *s(t)* from all *J* epochs is identical with the estimate from the two sub-averages:

$$s(t) = \frac{1}{2}(s_o(t) + s_e(t)) = \frac{1}{J}\sum_{j=1}^{J} x_j(t) \; . \quad (3)$$

The advantage of storing single epochs becomes apparent when the noise is estimated. Given all epochs, we can rigorously define and calculate the residual noise $\sigma(t)$ as the standard error of the average *s(t)*:

$$\sigma(t) = \sqrt{\frac{1}{J(J-1)}\sum_{j=1}^{J}(x_j(t) - s(t))^2} \; . \quad (4)$$

For data analysis we use the time-averaged quantities $s \equiv \mathrm{rms}(s(t))$, $\sigma_{oe} \equiv \mathrm{rms}(\sigma_{oe}(t))$, and $\sigma \equiv \mathrm{rms}(\sigma(t))$ as estimates of signal and noise rms, where rms(·) denotes the root mean square-value, i.e., the square root of the average across time of all squared samples.

The expected values of the estimates of the noise variances $\sigma^2$ and $\sigma_{oe}^2$ are the same:

$$\mathrm{E}(\sigma_{oe}^2) = \mathrm{E}(\sigma^2) = \frac{\sigma_0^2}{J} \; , \quad (5)$$

with $\sigma_0^2$ denoting the noise variance of the single epochs.

However, the variance of $\sigma_{oe}^2$ is greater by a factor $\frac{7}{4}J$ than the variance of $\sigma^2$:

$$\mathrm{var}(\sigma_{oe}^2) = \frac{7}{2}\frac{\sigma_0^4}{J^2} \; , \quad (6)$$

$$\mathrm{var}(\sigma^2) = 2\frac{\sigma_0^4}{J^3} \; . \quad (7)$$

A derivation of equations (5), (6) and (7) is given in the appendix.

The single-sweep-based SNR estimate $\gamma$ is given by

$$\gamma = \frac{s}{\sigma} \; , \quad (8)$$

while the average-based SNR estimate $\gamma_{oe}$ is analogously defined by

$$\gamma_{oe} = \frac{s}{\sigma_{oe}} \; . \quad (9)$$

Note that $\gamma$ and $\gamma_{oe}$ are dimensionless.

Another single-sweep-based quality measure, the so-called $F_{sp}$-value, was introduced by *Elberling* and *Don* (1984). It is basically the square of $\gamma$ as defined here with the denominator evaluated at a particular time sample $t_{sp}$ only: $F_{sp} = \gamma^2(t_{sp}) = s^2 / \sigma^2(t_{sp})$. *Elberling* and *Don* have shown that $F_{sp}$ does not depend significantly on the choice of the single time point. It is therefore frequently used to save computation time.

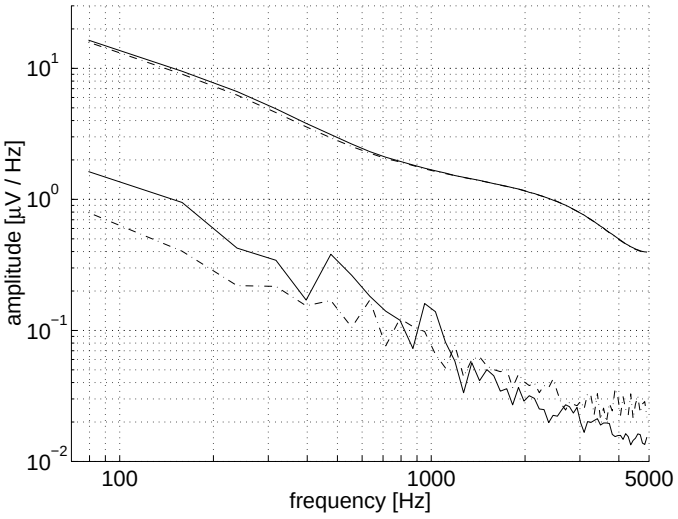


*Fig. 1: Upper curves: Average magnitude spectrum of single noise sweeps (dashed line) and single sweeps containing an ABR (solid line, response to binaural stimulation at 60 dB nHL); channel M2; 10,000 epochs per subject, averaged across subjects.*
*Lower curves: Spectra of averaged noise (dashed line) and response (solid line).*

*Abb. 1: Obere Kurven: Gemitteltes Amplitudenspektrum von Einzelepochen ohne Stimulation (gestrichelt) und mit diotischer Stimulation bei 60 dB nHL (durchgezogen) für Kanal M2. Mittel über Versuchspersonen und 10000 Epochen pro Versuchsperson.*
*Untere Kurven: Amplitudenspektren der gemittelten Einzelepochen ohne Stimulation (gestrichelt) und mit FAEP (durchgezogen).*

On the other hand, the average across time yields an estimate of the noise power with higher accuracy (variance divided by the number of samples per epoch) than a single-point variance. It is therefore used in this study and is also recommended for use in practical applications. *Cebulla* and collaborators, using Monte Carlo simulations, have recently shown an averaged »single point« variance to be superior to the classical $F_{sp}$, especially if the number of sweeps is low (*Cebulla* et al. 2000).

## 3. Results

Before applying any filters to the data, it is helpful to investigate the frequency composition of signal and noise without filtering[3].

Such a comparison between the spectrum of the signal and the average spectrum of the noise epochs is useful in order to derive an optimum filter characteristic, as all our filters are applied to the individual epochs before averaging. In order to obtain the respective spectra, the average magnitude spectrum was computed from unfiltered sets of no-stimulus sweeps and sweeps containing the response to 60 dB (nHL) binaural clicks from the nine subjects as follows:

The individual epochs were transformed into the frequency domain (discrete Fourier transform with $N = 125$, corresponding to 12.5 ms and a resolution of 80 Hz), and the *magnitudes* of these Fourier transforms were averaged. With this form of average, the mean strength of all components is the result irrespective of the respective phase characteristics. If the same quantity is computed for sweeps containing noise alone and noise plus evoked response, and if the number of sweeps is large enough, a comparison of the resulting spectra should allow the identification of signal frequency components[4].

The result is shown in the upper two curves of Fig. 1, where the average magnitude spectrum of the noise-only sweeps is the dashed line, and the solid line corresponds to noise plus signal (data for channel M2 and binaural stimulation at 60 dB (nHL), averaged across subjects). The two curves are indistinguishable above 1500 Hz and only exhibit very small differences below this frequency, indicating that the presence of the ABR adds very little energy. The two lower curves in the figure show the situation after averaging across the ensemble of epochs. As expected, the averaging process in the time domain has reduced the noise energy more than the respective signal energy. Most signal energy appears in the three bands from 80–400 Hz, 400–880 Hz, and 880–1200 Hz. These bands are separated by pronounced minima in the spectrum at approximately 400 and 880 Hz. Note that the frequency resolution is limited to 80 Hz due to the finite length of the ABR of 12.5 ms. Hence, the edge frequency estimates exhibit this variability and, in addition, the energy of signal and noise in the band from zero to 80 Hz is lumped together.

To give an idea of the effect of high and lowpass FIR filters on the waveform of the ABR, an example of data is shown for

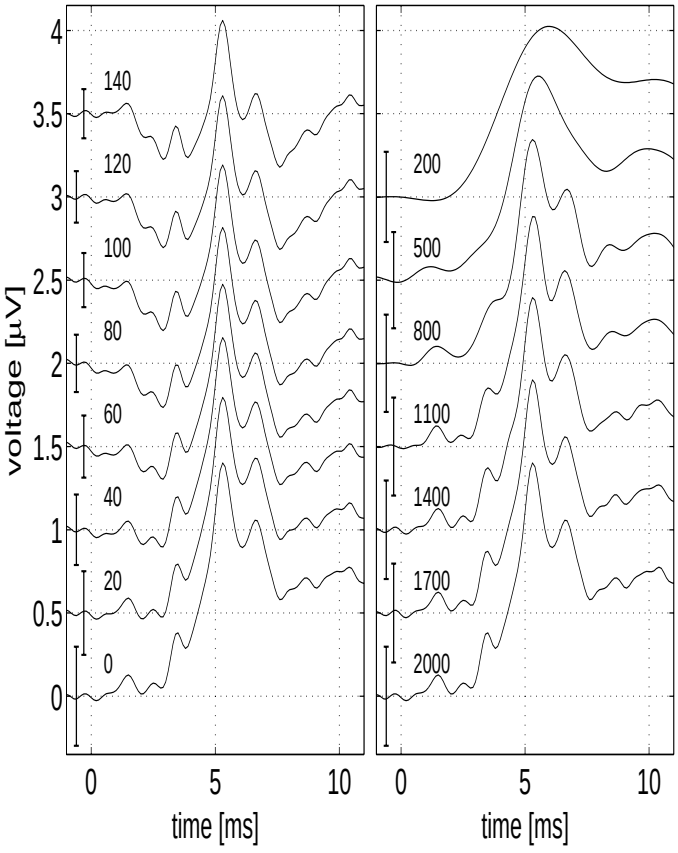


*Fig. 2: Effect of various highpass (left panel) and lowpass (right panel) filters on the waveform of the ABR for subject cr (diotic stimulation at 60 dB (nHL), channel M1). The lowermost graph is the same in both sub-plots: lowpass of 2 kHz only. The remaining curves (each shifted in the y-direction by 0.5 µV relative to the previons one) show the same data, but the highpass (left) and lowpass (right) is narrowed as indicated by the numbers above each graph. The vertical bar in the prestimulus interval indicates the averaged noise estimate.*

*Abb. 2: Einfluss verschiedener Hochpass- (links) und Tiefpasssfilter (rechts) auf das FAEP (Versuchsperson cr, diotische Stimulation bei 60 dB nHL, Kanal M1). Die unterste Kurve ist identisch in beiden Teilbildern und zeigt das breitbandige FAEP (0–2000 Hz). Im linken Bild erhöht sich nach oben die Hochpassgrenzfrequenz von 0 bis 140 Hz, im rechten Bild erniedrigt sich die Tiefpassgrenzfrequenz von 2000 bis 200 Hz. (Die Kurven sind mit 0.5 µV Abstand aufgetragen.) Der Fehlerbalken im Prästimulusintervall zeigt die Schätzung des Restrauschens.*

[3] Of course such an analysis can only be applied to *estimates* of both signal and noise.

[4] Here we make the approximation that the presence of the stimulus does not alter the spectral characteristics of the noise.

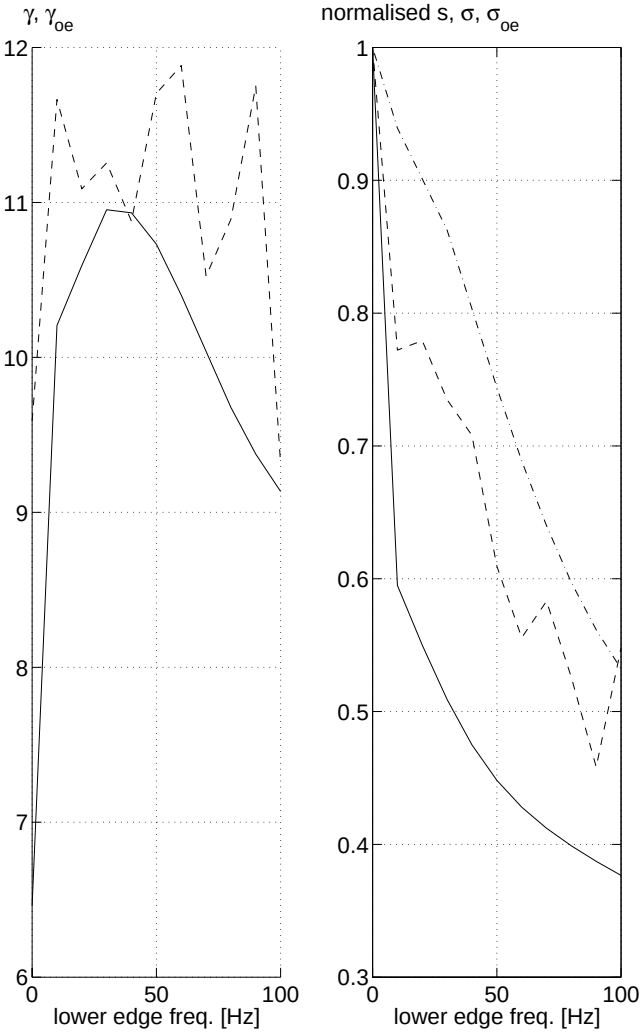


*Fig. 3: Left graph: the single-sweep-based SNR estimte $\gamma$ (eq. (8), solid line) as well as the average-based SNR estimate $\gamma_{oe}$, (eq. (9), dashed line) averaged across nine subjects as a function of the lower cut-off frequency.*
*Right graph: the common signal estimate s (eq. (3), dash-dotted line) and the noise estimates $\sigma$ (eq. (4), solid line) and $\sigma_{oe}$ (eq. (2), dashed line) normalized to their respective values for no highpass filter as a function of the lower cut-off frequency. Stimulus: binaural click at 60 dB (nHL);channel M2; averaging method: artifact threshold ±10 $\mu$V.*

*Abb. 3: Links: Die einzelepochenbasierte SNR-Schätzung $\gamma$ (Gl. (8), durchgezogen) und die mittelwertbasierte SNR-Schätzung $\gamma_{oe}$ (Gl. (9), gestrichelt) als Funktion der Hochpassgrenzfrequenz, Mittel über alle Versuchspersonen.*
*Rechts: Die gemeinsame Signalschätzung s (Gl. (3), gestrichpunktet), die einzelepochenbasierte Rauschschätzung $\sigma$ (Gl. (4), durchgezogen) und die mittelwertbasierte Rauschschätzung $\sigma_{oe}$ (Gl. (2), gestrichelt) als Funktion der Hochpassgrenzfrequenz. Die Werte sind normiert auf die entsprechenden Werte ohne Hochpassfilter. Stimulus: diotischer Click bei 60 dB nHL, Kanal M2, Mittelungsmethode: Artefaktschranke bei ±10 $\mu$V.*

one subject (cr, diotic stimulation at 60 dB (nHL), channel M1) in Fig. 2. In the left graph, the highpass cut-off frequency is raised from zero (no highpass) in steps of 20 Hz to 140 Hz (uppermost curve) while the lowpass is unchanged at 2000 Hz (1/5 of the sampling frequency). Analogously, in the right graph the lowpass cut-off frequency is lowered from 2000 Hz to 200 Hz in steps of 300 Hz (no highpass was applied to any of the curves). The vertical bar in the pre-stimulus interval shows the noise estimate. As the highpass becomes more restrictive, the residual noise decreases and the waveform exhibits less drift. As the lowpass is made more restrictive, first the highpass noise is removed and later, below about 1000 Hz, details of the signal are also filtered out. The lowpass has a much smaller effect on the residual noise.

Fig. 3 addresses the question of the lower cut-off frequency $f_l$. In the left graph the variation of the SNR estimates $\gamma$ and $\gamma_{oe}$ (as defined in Section 2.5) is shown for channel M2 and binaural stimulation at 60 dB (nHL) as a function of $f_l$ (the upper cut-off frequency, $f_u$, being held fixed at 2000 Hz). The data on which this figure is based were obtained by averaging with an artifact threshold of 10 $\mu$V. This is the most commonly used method and provides reliable estimates (cf. part II of the present study, *Riedel* et al. 2001). The values of the quality estimates $\gamma$ and $\gamma_{oe}$, shown in the left sub-plot of Fig. 3, are the quotients of the averages across subjects of the respective signal and noise estimates.[5]

While $\gamma$ shows a single maximum between 30 and 40 Hz, the average-based SNR estimate $\gamma_{oe}$ exhibits four maxima and provides no unambiguous value for an optimal cut-off frequency. The maximum of $\gamma$ can also be located from the right graph of the

[5] Note that this procedure gives a higher weighting to subjects with a large SNR. Normalising $\gamma$ prior to averaging eliminates this bias, but does not alter the location of the maximum and only has a small effect on the shape of the curve.

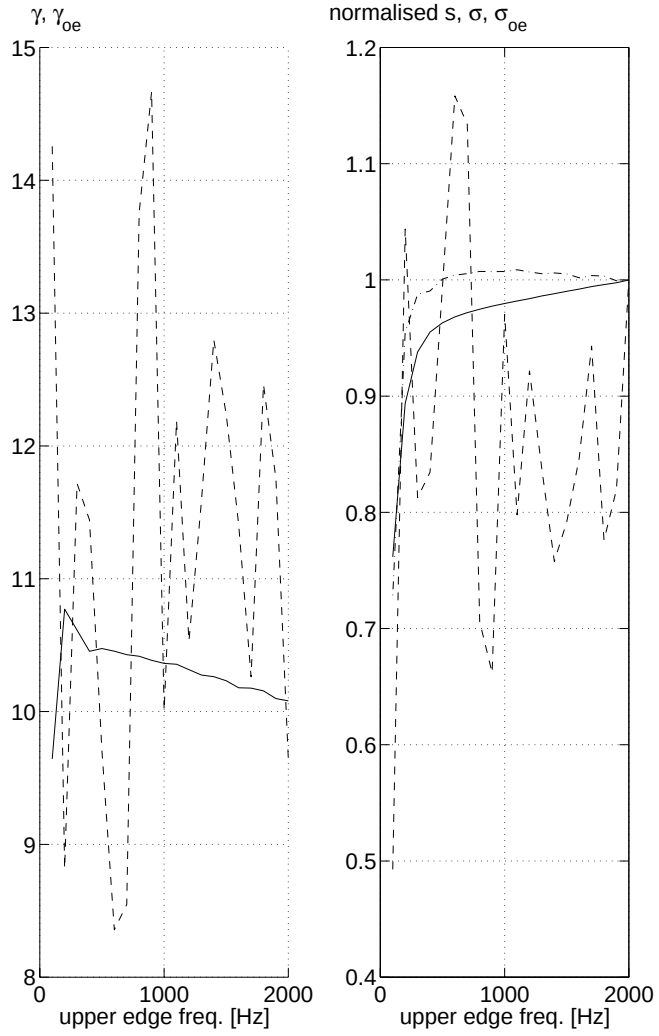


*Fig. 4: Left graph: the single-sweep-based SNR estimate $\gamma$ (eq. (8), solid line) as well as the average-based SNR estimte $\gamma_{oe}$ (eq. (9), dashed line) averaged across nine subjects as a function of the upper cut-off frequency.*
*Right graph: the common signal estimate s (eq. (3), dash-dotted line) and the noise estimates $\sigma$ (eq. (4), solid line) and $\sigma_{oe}$ (eq. (2), dashed line) normalized to their respective values at 2000 Hz as a function of the upper cut-off frequency. Stimulus: click at 60 dB (nHL); channel: M2; averaging method: artifact threshold ±10 $\mu$V.*

*Abb. 4: Links: Die einzelepochenbasierte SNR-Schätzung $\gamma$ (Gl. (8), durchgezogen) und die mittelwertbasierte SNR-Schätzung $\gamma_{oe}$ (Gl. (9), gestrichelt) als Funktion der Tiefpassgrenzfrequenz, Mittel über alle Versuchspersonen.*
*Rechts: Die gemeinsame Signalschätzung s (Gl. (3), gestrichpunktet), die einzelepochenbasierte Rauschschätzung $\sigma$ (Gl. (4), durchgezogen) und die mittelwertbasierte Rauschschätzung $\sigma_{oe}$ (Gl. (2), gestrichelt) als Funktion der Tiefpassgrenzfrequenz. Die Werte sind normiert auf die entsprechenden Werte für den Tiefpass mit 2000 Hz. Stimulus: diotischer Click bei 60 dB nHL, Kanal M2, Mittelungsmethode: Artefaktschranke bei ±10 $\mu$V.*

figure: here, the rms values of the signal (dash-dotted line) and noise (solid line) estimates are depicted separately as a function of the lower cut-off frequency. Additionally, the average-based noise estimate $\sigma_{oe}$ is shown (dashed line). The curves are normalized to the values obtained when no highpass filter is applied and only the DC-value of each epoch is subtracted (labelled $f_l$ = 0 Hz in the figure). Both quantities decrease rapidly as the cut-off frequency rises to $f_l$ = 10 Hz, but the noise rms declines more sharply than the signal rms, indicating that there is relatively more noise in the band from zero to 10 Hz than there is signal. This relation changes between 40 and 50 Hz. If the lower cut-off frequency is increased further, more signal energy than noise energy is eliminated. This makes higher values of $f_l$ unfavorable.

The issue of upper cut-off frequency is addressed in Fig. 4. Here, the same quantities as in Fig. 3 are shown, but as a function of the upper cut-off frequency $f_u$ (no highpass filter was employed). Although in the left graph there is a local maximum at 600 Hz, the maximum value of $\gamma$ is located at the unexpectedly low *upper* cut-off frequency of $f_u$ = 200 Hz. $\gamma_{oe}$ behaves entirely erratically and, again, is unsuitable for determining an optimal edge frequency. The right graph shows the signal and noise rms values, normalized to their respective values at $f_u$ = 2000 Hz. While the noise estimate $\sigma$ declines as the upper cut-off frequency is lowered (solid line), the signal rms *rises* by about two percent to $f_u$ = 1100 Hz before decreasing as signal energy is filtered out (dash-dotted line). This phenomenon is due to the application of an artifact rejection *after* filtering: Obviously, a number of sweeps exhibit both a high signal energy and a high peak-to-peak voltage. The latter exceeds the artifact threshold and excludes them from the average in the condition with high upper cut-off frequency. If the upper cut-off frequency is lowered, the artifact threshold is no longer exceeded, and hence the signal energy contained in these sweeps will enter the average signal and increase its rms value. Consequently, the energy of the average in this band will be *higher* than in the previous case, although

the lowpass is now stricter. The observation that the increase in *s* disappears if no artifact criterion is applied further supports this notion (data not shown). The irregular behaviour of the average-based quality estimate $\gamma_{oe}$ is due to the fluctuations of $\sigma_{oe}$ (dashed line).

The upper two graphs in Fig. 5 show the dimensionless SNR estimate $\gamma$ averaged across subjects, stimuli and presentation levels for the three channels as a function of lower and upper cut-off frequencies, respectively. The two mastoidal channels show almost identical characteristics with maxima at 40 Hz for $f_l$ and 200 Hz for $f_u$, whereas for Fz $\gamma$ peaks at 10 Hz and 100 Hz for lower and upper cut-off frequencies, respectively.

The two graphs in the middle row of Fig. 5 show $\gamma$ averaged across subjects, stimuli and channels for the three stimulation levels as a function of lower and upper cut-off frequencies, respectively. The SNR decreases with decreasing stimulation level. The drop from 40 to 20 dB is larger than that from 60 to 40 dB, reflecting the well-known non-linearity of the level-response characteristic of early auditory evoked potentials. The location of the optimal lower cut-off frequency is negligibly affected by the stimulation level (40 Hz for 20 dB, 30 Hz for 40 and 60 dB), whereas the maxima of $\gamma$ as a function of the upper cut-off frequency are at 500, 100, and 200 Hz for 20, 40, and 60 dB, respectively.

The lower two graphs in the same figure show the effect of stimulus type on the dependence of $\gamma$ on cut-off frequencies. The location of the maximum does not depend on stimulus type. The absolute value of the signal-to-noise ratio is larger for binaural stimulation than for monaural stimulation, but not doubled.

The effect of filtering varies significantly between subjects, as is shown in Figs. 6 and 7. Depending on the subject, the optimal lower cut-off frequency $f_l$ is found to be zero, 10, 30, 40 or 50 Hz, while the optimal upper cut-off frequency $f_u$ varies between 100 and 700 Hz. Note that the overall change in the signal-to-noise ratio induced by lowpass filtering is small: in terms of the SNR it is almost irrelevant if one uses $f_u$ = 500 Hz or $f_u$ = 2000 Hz. The low values of $f_u$ that optimize the SNR are unexpected, given the fact that the ABR contains energy above 1000 Hz. An upper cut-off frequency of 200 Hz leaves a barely recognisable, very smooth ABR. The reason for these low values will be discussed below. The choice of the lower cut-off frequency, on the other hand, can have a considerable impact on the SNR. The direction of this impact is, however, contrary for different subjects. For example, the increase of $f_l$ from 10 Hz to 100 Hz lowers the SNR for subject mg by almost 50 %, but increases the SNR by about 50 % for subject jt.

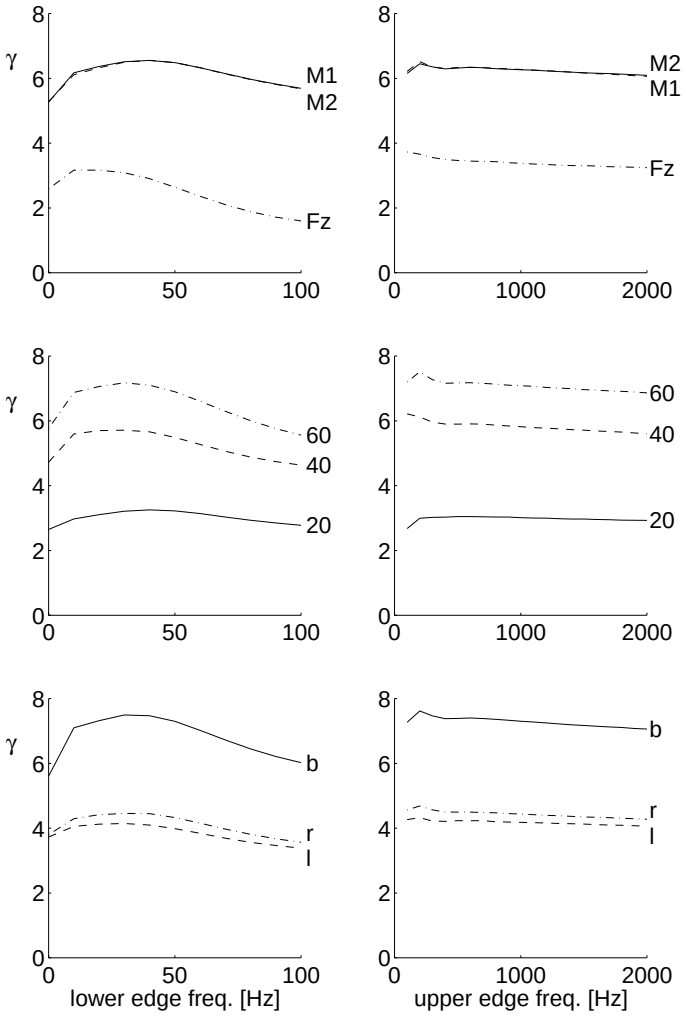


*Fig. 5: The SNR estimiate $\gamma$ (eq. (8)) as a function of lower (left column) and upper (right column) cut-off frequency.*
*Top row: $\gamma$ averaged across subjects, levels and stimuli for the channels M1, M2 and Fz.*
*Middle row: $\gamma$ averaged across subjects, channels and stimuli for the levels 20, 40, and 60 dB.*
*Bottom row: $\gamma$ averaged across subjects, levels and channels for monotic left (»l«), monotic right (»r«), and for binaural (»b«) stimulation. Averaging method: Artifact threshold ±10 $\mu$V.*

*Abb. 5: Geschätzter SNR ($\gamma$) als Funktion der unteren (linke Spalte) und oberen (rechte Spalte) Grenzfrequenz.*
*Oben : $\gamma$ gemittelt über Versuchspersonen, Pegel und Stimuli für die Kanäle M1, M2 und Fz.*
*Mitte: $\gamma$ gemittelt über Versuchspersonen, Kanäle und Stimuli für die Pegel 20, 40 und 60 dB nHL.*
*Unten: $\gamma$ gemittelt über Versuchspersonen, Pegel und Kanäle für monaural linke (»l«), monaural rechte (»r«) und binaurale (»b«) Stimulation.*

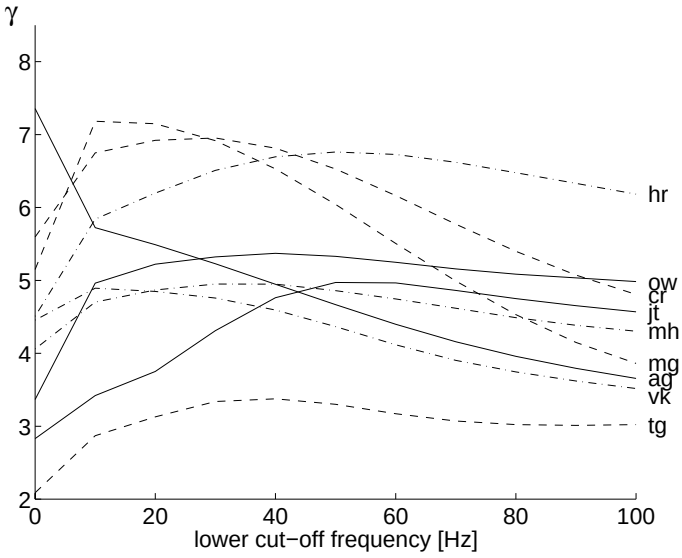


*Fig. 6: Estimated signal-to-noise ratios γ (according to eq. (8)) averaged across levels, stimuli and channels as a function of the lower cut-off frequency for each of the nine subjects. Averaging method: Artifact threshold ±10 μV.*

*Abb. 6: Geschätztes Signal-Rausch-Verhältnis γ (nach Gl. (8)) gemittelt über Pegel, Stimuli und Kanäle als Funktion der unteren Grenzfrequenz für alle neun Versuchspersonen. Mittelungsmethode: Artefaktschranke bei ±10 μV.*

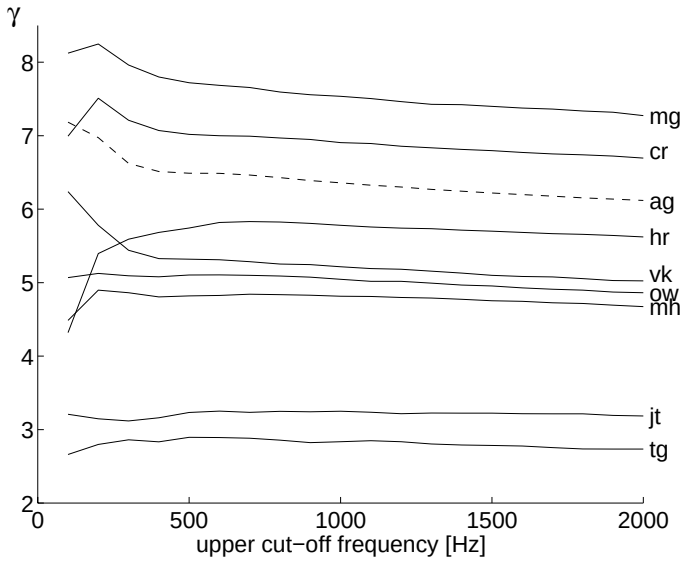


*Fig. 7: Estimated signal-to-noise ratios γ (according to eq. (8)) averaged across levels, stimuli and channels as a function of the upper cut-off frequency for each of the nine subjects. Averaging method: Artifact threshold ± 10 μV.*

*Abb. 7: Geschätztes Signal-Rausch-Verhältnis γ (nach Gl. (8)) gemittelt über Pegel, Stimuli und Kanäle als Funktion der oberen Grenzfrequenz für alle neun Versuchspersonen. Mittelungsmethode: Artefaktschranke bei ±10 γV.*

## 4. Discussion

The descriptions of the frequency composition of the ABR that can be found in the literature are contradictory. Usually, three bands are identified, but the gaps that separate them are located at different frequencies. *Elberling* (1979) reports gaps at 300 Hz and 600 Hz for responses to clicks at 105 dB (p.e. SPL), while *Møller* (1988) (who does not provide the level of the stimulus) finds them at 700 Hz and 1000 Hz, and *Pratt* et al. (1989) locate minima in the spectrum at 240 Hz and 484 Hz for clicks at 75 dB (nHL). None of these findings seem to agree with the spectrum shown in Fig. 1, which exhibits minima at 400 Hz and 880 Hz for 60 dB (nHL) clicks. Two aspects of these comparisons must be considered: firstly, given a recorded epoch of finite length, it is not possible to resolve the spectrum finer than the inverse of the recording interval. In our case, this spectral resolution amounts to 80 Hz, *Elberling* works with a resolution of 62.5 Hz, *Møller* with 98 Hz, and *Pratt* with 55 Hz, corresponding to recording intervals of 12.5 ms, 16 ms, 10.24 ms, and 18.2 ms, respectively. Secondly, the spectral composition of the ABR varies between subjects. While Fig. 1 shows data averaged across subjects, it is possible to find a particular subject with gaps in the spectrum at almost all the frequencies mentioned above (within the frequency resolution). In conclusion, the spectrum of the ABR is limited to the range below 1500 Hz, but any more detailed analysis is only valid for the particular subject under investigation.

Considering the large fluctuation of optimal lower cut-off frequencies for the different subjects depicted in Fig. 6, it seems to be questionable whether it is at all possible to recommend a specific highpass. In the literature, recommendations for digital highpass filters range from 30 Hz for infants (*Sininger* 1995) to 100 Hz (*Doyle* and *Hyde* 1981a; *Stockard* et al. 1978) to 150–200 Hz (*Tietze* and *Kevanishvili* 1990) through 400 Hz (*Mühler* and *von Specht* 1996) to *Elberling's* well-known recommendation to handle highpass filtering of ABR »with care« (*Elberling* 1979). The version for such variance may well be the strong inter-individual fluctuations in the data presented here. Note that most of the studies mentioned above did not use single-sweep-based estimates of the residual noise (except for *Mühler* and *von Specht* 1996) and *Sininger* (1995) as was done here. Thus, their SNR estimates for individual subjects exhibit a higher statistical variability than in our case, and a separation of inter-individual variability and noise statistics is more difficult. Hence, most studies base their recommendations for filter parameters on the *average* data across

subjects. The lack of consistency of cut-off frequencies across subjects could also be due to differences in the signal-to-noise ratio of the various subjects. However, even the subjects with high signal-to-noise ratio in Figs. 6 and 7 show a strong variation of optimal cut-off frequencies. Since the highest optimal $f_l$ we find is 50 Hz, most of the common recommendations from the literature seem to be too high. The IFCN recommended standard is 60 Hz (*Nuwer* et al. 1994), slightly higher, but basically in agreement with our results. However, the justifications of the recommendations found in the literature differ from ours. Some are based on the extent to which filtering affects wave latencies (*Mühler* and *von Specht* 1996) or Jewett *V* peak-to-peak voltages (*Sininger* 1995) or lead to results that can be compared with clinical normative data (*Stockard* et al. 1978). Clinically, these are the most important characteristics of the ABR. However, the SNR plays a central role for those research applications which aim at the localization of equivalent sources (*Kavanagh* et al. 1978; *Okamoto* et al. 1983).

The lack of correlation of optimal highpass frequency with the stimulation level shown in the left graph of the middle row of Fig. 5 seems at first to be in contrast to the recommendations given in the literature, in particular with *Elberling's* (1979) finding that the main power of the ABR shifts to lower frequencies if the level is decreased. *Sininger* (1995) demonstrated that for neonates stimulated with clicks of 15 and 30 dB (nHL) and tone bursts of 40 and 60 dB (nHL), a 30 Hz highpass yields higher $F_{sp}$ values than a 100 Hz highpass (*Elberling* and *Don* 1984), but did not question the adequacy of the traditional 100 Hz setting for clicks of higher intensity. Apart from extending her findings to the responses of adults, our results show that even for clicks with levels as high as 60 dB (nHL), filter settings significantly lower than 100 Hz are advantageous.

Our method indicates that the lowpass cut-off frequency has a very minor effect on the SNR. Nevertheless, the fact that we find optimal *upper* cut-off frequencies of 200 Hz in some subjects is surprising. This finding can be explained as follows: if both the upper and the lower cut-off frequency were allowed to vary independently, one would find a global maximum for a filter condition which cuts out everything except for a single frequency bin, namely the bin in which the SNR is the highest. Including any other frequency component in the average would clearly decrease the SNR. In fact a threshold of 200 Hz is in agreement with *Elberling's* result that the main power of the ABR is located below 250 Hz (*Elberling* 1979). This does not permit the conclusion, however, that such a filter is optimal because there definitely *is* signal in other frequency bins (remember the curve in the upper right corner of Fig. 2, which is barely recognizable as an ABR). Therefore, the goal should be to include all those frequency components where there is more signal energy than noise energy. The relative amount of signal versus noise energy varies, however, with the number of sweeps processed. In consequence, the optimal cut-off frequencies change in the course of averaging as the residual noise decreases below the signal energy in the various frequency bins. In other words, apart from the inter-individual variation of the frequency composition of noise and signal, cut-off frequencies also depend on the number of sweeps recorded. The more epochs the average includes, the broader the frequency band that adds information to the average[6] will be. For an ensemble with $J$ = 10,000 sweeps (as used in our experiments), a reduction of the noise by roughly a factor of 100 can be expected. With this assumption, 1500 Hz, 1100 Hz, and 950 Hz are found to be the ideal upper cut-off frequencies for channels M1, M2, and Fz, respectively. These values are in agreement with the recommendations given in the literature (*Boston* and *Ainslie* 1980; *Doyle* and *Hyde* 1981a; *Mühler* and *von Specht* 1996; *Møller* 1988) and with clinical practice. Only a few authors (*Stockard* et al 1978; *Nuwer* et al. 1994) recommend lowpass cut-off values of 3000 Hz.

## 5. Conclusions

- As demonstrated both theoretically and empirically in its regular dependence on the lower and upper cut-off frequency, the single-sweep-based SNR estimate ($\gamma$) used in the present study gives a more stable and valid estimate of the properties of the auditory brain stem response than the conventional average-based estimate ($\gamma_{oe}$).
- The reason for the superiority of $\gamma$ is that the variance of its corresponding noise estimate is smaller than the variance of the average-based noise estimate by a factor proportional to the number of epochs that entered the average.
- The optimum linear filter settings do not vary significantly with stimulus level, but show considerable variation across subjects.
- The cut-off frequency $f_l$ of the high-pass filter should not exceed 50 Hz.
- The cut-off frequency $f_u$ of the low-pass filter only exerts a small influence on the SNR. It should be set at 1300 to 1700 Hz.

[6] Theoretically it is conceivable that, below a certain number of sweeps, there is a gap in the »ideal« passband, which closes as more sweeps are accepted. Considering the upper two curves of Fig. 1, however, such a scenario does not seem likely.

## Appendix

Here all quantities are treated as time independent, i.e., for one time sample only. However, the results are the same for each sample in time. Similar results hold for the time-averaged quantities.

To prove equations (5), (6) and (7), the following assumptions have to be fulfilled:

- From the measured values $x_j$, $j = 1,...J$, a signal estimate $s$, cf. eq. (3), is obtained, which is a random variable. From $s$, the corresponding noise estimates $n_j = x_j - s$, $j = 1,...J$ can be derived. They are also random variables.
- The measured values $x_j$ consist of a reproducible signal $S$ and a random additive noise $N_j$ : $x_j = S + N_j$.
- The noise values are realisations of a random variable $N_j$ that obey a Gaussian distribution with zero mean and variance $\sigma_0^2$.
- Noise values $N_j$ and $N_k$ are uncorrelated for all epochs where $j \neq k$.

According to eq. (2), the average-based estimate of the noise variance is

$$\sigma_{oe}^2 = \frac{1}{4}(s_o - s_e)^2 = \frac{1}{4}\Big(S + \frac{2}{J}\sum_{o=1,3,...}^{J-1} N_o - S - \frac{2}{J}\sum_{e=2,4,...}^{J} N_e\Big)^2 = \frac{1}{J^2}\Big(\sum_o N_o - \sum_e N_e\Big)^2 \quad (10)$$

Given the independence of the noise values, i.e. $E(N_jN_k) = E(N_j)E(N_k)$, the expectation value of $\sigma_{oe}^2$ can be written as

$$\begin{aligned} E(\sigma_{oe}^2) &= \frac{1}{J^2}\Big\{E\Big((\sum_o N_o)^2\Big) - 2E\Big(\sum_o N_o \sum_e N_e\Big) + E\Big((\sum_e N_e)^2\Big)\Big\} \\ &= \frac{1}{J^2}\Big\{\sum_o E(N_o^2) - 2E\Big(\sum_o N_o\Big)E\Big(\sum_e N_e\Big) + \sum_e E(N_e^2)\Big\} \\ &= \frac{1}{J^2}\Big\{\frac{J}{2}\sigma_0^2 - 0 + \frac{J}{2}\sigma_0^2\Big\} = \frac{\sigma_0^2}{J}\,. \end{aligned} \quad (11)$$

According to eq. (4), the single-sweep-based estimate of the noise variance is

$$\sigma^2 = \frac{1}{J(J-1)}\sum_{j=1}^{J}(x_j - s)^2 = \frac{1}{J(J-1)}\sum_{j=1}^{J} n_j^2\,. \quad (12)$$

The division by $J(J-1)$ is necessary because $s$ is the signal estimate, not the true signal $S$. Without loss in generality, however, we may assume that the true signal $S$ is known. Since this assumption provides an extra degree of freedom, we derive

$$\sigma^2 = \frac{1}{J^2}\sum_{j=1}^{J}(x_j - S)^2 = \frac{1}{J^2}\sum_{j=1}^{J} N_j^2\,. \quad (13)$$

The expectation value of the single-sweep-based estimate of the noise variance is

$$E(\sigma^2) = \frac{1}{J^2}E\Big(\sum_{j=1}^{J} N_j^2\Big) = \frac{1}{J^2}\sum_{j=1}^{J} E(N_j^2) = \frac{1}{J^2}\sum_{j=1}^{J}\sigma_0^2 = \frac{\sigma_0^2}{J}\,. \quad (14)$$

With the above, the equality of the expectation values of both noise estimates (eq. (5)) is proven. The result reflects the well-known fact that during the averaging process, noise variance is reduced by the number of epochs entering the average.

The crucial difference between $\sigma_{oe}^2$ and $\sigma^2$ is their respective variance. To derive these quantities, the kurtosis of the sum of normally distributed random variables with variance $\sigma_0^2$ is needed. With the identity

$$\int_0^\infty x^m e^{-ax^2}dx = \frac{\Gamma(\frac{m+1}{2})}{2a^{(\frac{m+1}{2})}} \quad , a > 0,\ m > -1 \quad (15)$$

and setting $a = 1/(2\sigma_0^2)$ and $m = 4$, for $J = 1$ we get

$$E(N^4) = \frac{1}{\sqrt{2\pi}\sigma_0}\int_{-\infty}^{\infty} N^4 e^{-\frac{N^2}{2\sigma_0^2}}dN = \frac{2}{\sqrt{2\pi}\sigma_0}\Gamma\Big(\frac{5}{2}\Big)\frac{1}{2}(2\sigma_0^2)^{5/2} = 3\sigma_0^4\,. \quad (16)$$

Since only quadratic terms in $N_j$ contribute to the expectation value, for the sum of $J/2$ terms we get

$$\begin{aligned} E\Big\{(\sum_{j=1}^{J/2} N_j)^4\Big\} &= E\Big\{\sum_{j=1}^{J/2} N_j^4 + \sum_{j=1}^{J/2}\sum_{\substack{k=1\\k\neq j}}^{J/2}\binom{4}{2} N_j^2 N_k^2\Big\} \\ &= \sum_{j=1}^{J/2} E(N_j^4) + 6\sum_{j=1}^{J/2}\sum_{\substack{k=1\\k\neq j}}^{J/2} E(N_j^2)E(N_k^2) \\ &= \frac{J}{2}3\sigma_0^4 + 6\frac{J}{2}\Big(\frac{J}{2} - 1\Big)\sigma_0^2\sigma_0^2 \\ &= \frac{3}{2}J(J-1)\sigma_0^4\,. \end{aligned} \quad (17)$$

Using this result and assuming $J >> 1$, the variance of the average-based estimate of the noise variance can be calculated:

$$\begin{aligned} \mathrm{var}(\sigma_{oe}^2) &= E((\sigma_{oe}^2)^2) - (E(\sigma_{oe}^2))^2 = E(\sigma_{oe}^4) - \frac{\sigma_0^4}{J^2} \\ &= \frac{1}{J^4}E\Big\{(\sum_o N_o - \sum_e N_e)^4\Big\} - \frac{\sigma_0^4}{J^2} \\ &= \frac{1}{J^4}\Big\{E\Big((\sum_o N_o)^4\Big) - 4E\Big((\sum_o N_o)^3(\sum_e N_e)\Big) + 6E\Big((\sum_o N_o)^2(\sum_e N_e)^2\Big) \\ &\quad -4E\Big((\sum_o N_o)(\sum_e N_e)^3\Big) + E\Big((\sum_e N_e)^4\Big)\Big\} - \frac{\sigma_0^4}{J^2} \\ &= \frac{1}{J^4}\Big\{\frac{3}{2}J(J-1)\sigma_0^4 + 6\Big(\frac{J}{2}\sigma_0^2\Big)\Big(\frac{J}{2}\sigma_0^2\Big) + \frac{3}{2}J(J-1)\sigma_0^4\Big\} - \frac{\sigma_0^4}{J^2} \\ &= \frac{\sigma_0^4}{J^2}\Big(\frac{7}{2} - \frac{3}{J}\Big) \approx \frac{7}{2}\frac{\sigma_0^4}{J^2}\,. \end{aligned} \quad (18)$$

On the other hand, the variance of the single-sweep-based estimate of the noise variance is

$$\begin{aligned}\mathrm{var}(\sigma^2) &= \mathrm{E}((\sigma^2)^2) - (\mathrm{E}(\sigma^2))^2 \\ &= \frac{1}{J^4}\,\mathrm{E}\Big\{(\sum_{j=1}^{J} N_j^2)(\sum_{k=1}^{J} N_k^2)\Big\} - \frac{\sigma_0^4}{J^2} \\ &= \frac{1}{J^4}\Big(\sum_{j=1}^{J}\mathrm{E}(N_j^4) + \sum_{j=1}^{J}\sum_{\substack{k=1\\k\neq j}}^{J}\mathrm{E}(N_j^2)\,\mathrm{E}(N_k^2)\Big) - \frac{\sigma_0^4}{J^2} \\ &= \frac{1}{J^4}\Big(3J\sigma_0^4 + J(J-1)\sigma_0^2\sigma_0^2\Big) - \frac{\sigma_0^4}{J^2} \\ &= 2\,\frac{\sigma_0^4}{J^3}\,.\end{aligned} \tag{19}$$

These derivations prove equations (6) and (7). Expectation value and variance of the single-sweep-based noise variance estimate can also be derived by noting that

$$\sigma^2 = \frac{\sigma_0^2}{J^2}\sum_{j=1}^{J}\left(\frac{N_j}{\sigma_0}\right)^2 . \tag{20}$$

The sum in the above equation obeys a $\chi^2$-distribution with $\nu = J$ degrees of freedom, and therefore has expectation value $J$ and variance $2J$, which is consistent with equations (14) and (19).

## Acknowledgements

This study was supported by the *Deutsche Forschungsgemeinschaft* as part of the *Sonderforschungsbereich Neurokognition* (SFB 517).

## References/Literatur

*Boston JR, Ainslie PJ* (1980) Effects of analog and digital filtering on brain stem auditory evoked potentials. Electroenceph clin Neurophysiol 48, 361–364

*Cebulla M, Stürzebecher E, Wernecke KD* (2000) Untersuchung verschiedener SNR-Schätzer für den Nachweis von biologischen Reizantworten im Rauschen. Z Audiol 39(1), l4–22

*Dawson WW, Doddington HW* (1973) Phase distortion of biological signals: extraction of signal from noise without phase error. Electroenceph clin Neurophysiol 34, 207–211

*Doyle DJ, Hyde ML* (1981a) Analogue and digital filtering of auditory brainstem responses. Scand Audiol 10, 81–89

*Doyle DJ, Hyde ML* (1981b) Bessel filtering of brain stem auditory evoked potentials. Electroenceph clin Neurophysiol 51, 446–448

*Elberling C* (1979) Auditory electrophysiology: spectral analysis of cochlear and brain stem evoked potentials. Scand Audiol 8, 57–64. Letter to the editor

*Elberling C, Don M* (1984) Quality estimation of averaged auditory brainstem responses. Scand Audiol 13, 187–197

*Elton M, Scherg M, von Cramon D* (1984) Effects of high-pass filter frequency and slope on BAEP amplitude, latency and wave form. Electroenceph clin Neurophysiol 57(5), 490–494

*Janssen R, Benignus VA, Grimes LM, Dyer RS* (1986) Unrecognized errors due to analog filtering of the brain-stem auditory evoked response. Electroenceph clin Neurophysiol 65, 203–211

*Jasper HH* (1975) The ten twenty electrode system of the international federation. Electroenceph clin Neurophysiol 10, 371–375, Appendix

*Kavanagh RN, Darcey TM, Lehmann D, Fender DH* (1978) Evaluation of methods for three-dimensional localization of electrical sources in the human brain. IEEE Trans Biomed Eng 25(5), 421–429

*Mühler R, von Specht H* (1996) Digitale Einzelsweep-Filterung früher auditorisch evozierter Potentiale. Z Audiol 35, 12–20

*Møller AR* (1988) Use of zero-phase digital filters to enhance brain-stem auditory evoked potentials (baeps). Electroenceph clin Neurophysiol 71, 226–232

*Nuwer MR, Aminoff M, Goodin D, Matsuoka S, Mauguière F, Starr A, Vibert JF* (1994) Ifcn recommanded standards for brain-stem auditory evoked potentials. Report of an ifcn committee. Electroenceph clin Neurophysiol 91, 12–17

*Okamoto Y, Teramachi Y, Musha T* (1983) Limitation of the inverse Problem in body surface potential mapping. IEEE Trans Biomed Eng 30(11), 749–54

*Oppenheim AV, Schaefer RW* (1989) Digital Signal Processing Series. Prentice-Hall, Englewood Cliffs, NJ, 07632

*Pratt H, Urbach D, Bleich N* (1989) Auditory brainstem evoked potentials peak identificattion by finite impulse response digital filters. Audiology 28, 272–283

*Riedel H, Granzow M, Kollmeier B* (2001) Single-sweep-based methods to improve the quality of auditory brain stem responses. Part II: averaging methods. Z Audiol, accepted, in press

*Schimmel H* (1967) The (±) reference: accuracy of estimated mean components in average response studies. Science 157, 92–93

*Sininger YS* (1995) Filtering and spectral characteristics of averaged auditory brain-stem response and background noise in infants. J Acoust Soc Am 98(4), 2048–2055

*Stockard JJ, Stockard JE, Sharbrough FW* (1978) Nonpathologic factors influencing brainstem auditory evoked potentials.Am J EEG Technology 18, 177–209

*Tietze G, Kevanishvili Z* (1990) Frequenzzusammensetzung und Filterung des frühen akustisch evozierten potentials (FAEP). HNO 38, 399–407

*Wong PKH, Bickford RG* (1980) Brain stem auditory evoked potentials: the use of noise estimate. Electroenceph clin Neurophysiol 50, 25–34